Structural Engineering and Mechanics, Vol. 31, No. 2 (2009) 117-135
DOI: http://dx.doi.org/10.12989/sem.2009.31.2.117

Effects of stiffness on reflection and transmission of micropolar thermoelastic waves at the interface between an elastic and micropolar generalized thermoelastic solid

Rajneesh Kumar†

Department of Mathematics, Kurukshetra University, Kurukshetra, India

Nidhi Sharma and Paras Ram

Department of Mathematics, N I T, Kurukshetra 136119, India

(Received October 20, 2006, Accepted December 4, 2008)

Abstract. The reflection and transmission of micropolar thermoelastic plane waves at the interface between an elastic solid and micropolar generalized thermoelastic solid is discussed. The interface boundary conditions obtained contain interface stiffness (normal stiffness and transverse stiffness). The expressions for the reflection and transmission coefficients which are the ratios of the amplitudes of reflected and transmitted waves to the amplitude of incident waves are obtained for normal force stiffness, transverse force stiffness and welded contact. Numerical calculations have been performed for amplitude ratios of various reflected and transmitted waves. The variations of amplitude ratios with angle of incident wave have been depicted graphically. It is found that the amplitude ratios of reflected and transmitted waves are affected by the stiffness, micropolarity and thermal distribution of the media.

Keywords: micropolar generalized thermoelastic solid; normal force stiffness; transverse force stiffness; welded contact; amplitude ratios.

1. Introduction

The exact natures of layers beneath the earth's surface are unknown. One has, therefore, to consider various appropriate models for the purpose of theoretical investigation.

The linear theory of elasticity is of paramount importance in the stress analysis of steel, which is the commonest engineering structural material. To a lesser extent linear elasticity describes the mechanical behavior of other common solid materials, e.g., concrete, wood and coal. However, the theory does not apply to the behavior of many of the new synthetic material of the elastomer and polymer type, e.g., polymethyl-methacrylate (Perspex), polyethylene, polyvinyl chloride.

Theory of micropolar continua was proposed by Eringen and Suhubi (1964) and Eringen (1968) to describe the continuum behavior of materials possessing microstructure. Basically, the difference

† Ph.D., Corresponding author, E-mail: rajneesh_kuk@rediffmail.com

between classical continuum theories and that of micropolar continuum theory is that the later admits independent rotations of the materials substructure; that is, the local intrinsic rotations (micro-rotations) which are taken to be kinematically independent of the linear displacements. It is believed that such a theory is applicable in the treatment of granular and fibrous composite materials.The granular nature of the material, microstructure becomes important in transmitting waves of small wave length and/or high frequency because they may reveal new types of waves not encountered in the classical theory of elasticity. Even when grain size is not visible to the eye if the wave length is comparable with the average grain size, the motion of the grains must be taken into account. In such cases, the local micromotion may in fact become dominant.

In recent years there has been much written on the subject of the theory of micropolar thermoelasticity. A comprensive review of works on the subject was given by Eringen (1970, 1999) and Nowacki (1966). Boschi and Iesan (1973) extended a generalized theory of micropolar thermoelasticity that permits the transmission of heat as thermal waves at finite speed.

Imperfect bonding considered in the present investigation is to mean that the stress components, heat flux are continuous and the small displacement field, temperature are not. The small vector difference in the displacement is assumed to depend linearly on the traction vector and in temperature it is assumed to depend linearly on heat flux. Some applications of such a generalization to electrodynamics problems are the study of composite media, crack detection and seismic wave propagation.

Significant work has been done to describe the physical conditions on the interface by different mechanical boundary conditions by different investigators. Notable among them are Jones and whitter (1967), Murty (1975), Nayfeh and Nassar (1978), Schoenberg (1980), Rokhlin *et al.* (1980), Rokhlin (1984), Pilarski and Rose (1988), Baik and Thompson (1984), Achenbach and coauthors (1985, 1988) and Lavrentyev and Rokhlin (1998).

Recently various authors have used the imperfect conditions at the interfaceto study various types of problems (Fan and Sze 2001, Wang and Zhong 2003, Chen *et al.* 2004, Shodja *et al.* 2006, Samanshariat and Eslami 2006).

Kumar and Singh (1996, 1998) discussed various problems on wave propagation in micropolar generalized thermoelastic solid. Kumar (2000) discussed the wave propagation in a micropolar viscoelastic generalized thermoelastic solid. Sharma *et al.* (2003) studied the reflection of generalized thermoelastic waves from the boundary of a half-space. Kumar and Sharma (2005) discussed the reflection of plane waves from the boundaries of a micropolar thermoelastic half-space without energy dissipation. Othman *et al.* (2006) investigated the effect of rotation on the reflection of magneto-thermoelastic waves under thermoelasticity without energy dissipation. Kumar and Sarthi (2006) studied the reflection and refraction of thermoelastic plane waves using the imperfect conditions at an interface between two thermoelastic media without energy dissipation. Recently Kumar *et al.* (2006) investigated the reflection and transmission of micropolar elastic waves at an imperfect boundary.

In the present investigation, the reflection and transmission at an imperfect interface between two dissimilar homogeneous, isotropic micropolar elastic half-spaces when micropolar thermoelastic waves (longitudinal displacement wave (LD-wave) or thermal wave (T-wave)or a set of coupled transverse displacement and transverse microrotational waves (CD I and CD II- waves) are incident at the interface. The amplitude ratios for various reflected and transmitted waves have been calculated for an imperfect boundary and deduced for normal force stiffness (NS), transverse force stiffness (TS) and welded contact (WC). The variations of amplitude ratios with angle of incidence are presented graphically to show the effect of stiffness, micropolarity and thermal distribution of the media.

2. Basic equations

Following Eringen (1968) and Lord and Shulman (1970), the constitutive relations and equations of the motion in micropolar generalized thermoelastic solid in absence of body forces, body couples and heat sources are given by

$$t_{kl} = \lambda u_{r,r}\delta_{kl} + \mu(u_{k,l} + u_{l,k}) + K(u_{l,k} - \varepsilon_{klr}\phi_r) - \upsilon T\delta_{ij} \tag{1}$$

$$m_{kl} = \alpha\phi_{r,r}\delta_{kl} + \beta\phi_{k,l} + \gamma\phi_{l,k} \tag{2}$$

$$(c_1^2 + c_3^2)\nabla(\nabla\cdot\vec{u}) - (c_2^2 + c_3^2)\nabla\times(\nabla\times\vec{u}) + c_3^2\nabla\times\vec{\phi} - \bar{\upsilon}\nabla T = \frac{\partial^2\vec{u}}{\partial t^2} \tag{3}$$

$$(c_4^2 + c_5^2)\nabla(\nabla\cdot\vec{\phi}) - c_4^2\nabla\times(\nabla\times\vec{\phi}) + \omega_0^2\nabla\times\vec{u} - 2\omega_0^2\vec{\phi} = \frac{\partial^2\vec{\phi}}{\partial t^2} \tag{4}$$

$$K^*\nabla^2 T = \rho C^*\left(\frac{\partial T}{\partial t} + \tau_0\frac{\partial^2 T}{\partial t^2}\right) + \upsilon T_0\left(\frac{\partial}{\partial t} + \tau_0\frac{\partial^2}{\partial t^2}\right)\nabla\cdot\vec{u} \tag{5}$$

where
$\lambda, \mu, K, \alpha, \beta, \gamma$ - material constants, ρ - density, j - microinertia, T - temperature distribution, $\vec{u}$ - displacement vector, $\vec{\phi}$ - microrotation vector, ε_{klr} - alternate tensor, K^* - thermal conductivity, t - time, C^* - specific heat at constant strain, $\upsilon-(3\lambda+2\mu+K)\alpha_t$, α_t - coefficient of linear thermal expansion, ε_{ij} - alternate tensor, t_{ij} - components of force stress tensor, m_{ij} - components of couple stress tensor, T_0 - reference temperature, τ_0 - relaxation time, δ_{ij} - Kronecker delta.

$$\nabla = \hat{i}\frac{\partial}{\partial x} + \hat{j}\frac{\partial}{\partial y} + \hat{k}\frac{\partial}{\partial z}, \quad \nabla^2 = \frac{\partial^2}{\partial x^2} + \frac{\partial^2}{\partial y^2} + \frac{\partial^2}{\partial z^2}$$

and

$$\left.\begin{aligned} & c_1^2 = \frac{\lambda + 2\mu}{\rho},\ c_2^2 = \frac{\mu}{\rho},\ c_3^2 = \frac{K}{\rho},\ c_4^2 = \frac{\gamma}{\rho_j},\ c_5^2 = \frac{\alpha+\beta}{\rho_j},\ \omega_0^2 = \frac{K}{\rho_j} \\ & \bar{\upsilon} = \frac{\upsilon}{\rho} \end{aligned}\right\} \tag{6}$$

3. Formulation and solution of the problem

We consider homogeneous, isotropic elastic solid and micropolar generalized thermoelastic solid half-spaces being in contact with each other at a plane surface which we designate as the plane $z = 0$ of a rectangular cartesian co-ordinate system OXYZ. We consider micropolar thermoelastic plane waves in xz-plane with wave front parallel to y-axis and all the field variables depend only on x, z and t.

For the two dimensional problem, the components of displacement and microrotation are given by

$$\vec{u} = (u_1, 0, u_3) \tag{7}$$

$$\vec{\phi} = (0, \phi_2, 0) \tag{8}$$

The components of displacement u_1, u_3 are related by the potential functions $q(x,z,t)$ and $\psi(x,z,t)$ as

$$u_1 = \frac{\partial q}{\partial x} - \frac{\partial \psi}{\partial z} \tag{9}$$

$$u_3 = \frac{\partial q}{\partial z} + \frac{\partial \psi}{\partial x} \tag{10}$$

Making use of Eqs. (7)-(10) in Eqs. (3)-(5) and assuming the time harmonic behavior as $\exp(i\omega t)$, we obtain

$$\left(\nabla^2 + \frac{\omega^2}{c_1^2 + c_3}\right) q - \bar{\upsilon} T = 0 \tag{11}$$

$$\left(\nabla^2 + \frac{\omega^2}{c_2^2 + c_3^2}\right) \psi + p\phi_2 = 0 \tag{12}$$

$$\left(\nabla^2 - 2q_0 + \frac{\omega^2}{c_4^2}\right) \phi_2 - q_0 \nabla^2 \psi = 0 \tag{13}$$

$$\bar{K}^* \nabla^2 T = C^* (1 + \tau_0 i\omega) i\omega T + \bar{\upsilon} T_0 (1 + \tau_0 i\omega) i\omega \nabla^2 q \tag{14}$$

where

$$\bar{K}^* = \frac{K^*}{\rho},\ \bar{\upsilon} = \frac{\upsilon}{\rho},\ p = \frac{K}{\mu + K},\ q_0 = \frac{K}{\gamma} \tag{15}$$

and ω is the circular frequency.

Substituting the value of T from Eq. (11) in Eq. (14), we obtain

$$(\nabla^4 + A\omega^2 \nabla^2 + B\omega^4) q = 0 \tag{16}$$

where

$$A = \frac{1}{c_1^2 + c_3^2} - \frac{i C^*}{\omega \bar{K}^*} \{(1 + i\omega\tau_0)(1 + \varepsilon)\} \tag{17}$$

$$B = -\frac{i}{\omega} \frac{C^*}{\bar{K}^* (c_1^2 + c_3^2)} (1 + \tau_0 i\omega) \tag{18}$$

and

$$\varepsilon = \frac{\overline{\upsilon}^2 T_0}{C^*(c_1^2 + c_3^2)}$$

Eliminating ϕ_2 from Eq. (12) and (13) we obtain following equations

$$(\nabla^2 + \omega^2 C\nabla^2 + \omega^4 D)\,\psi = 0 \tag{19}$$

where

$$C = \frac{q_0(p-2)}{\omega^2} + \frac{1}{(c_2^2 + c_3^2)} + \frac{1}{c_4^2}, \quad D = \left(\frac{1}{c_4^2} - \frac{2q_0}{\omega^2}\right)\frac{1}{c_2^2 + c_3^2} \tag{20}$$

We assume solution of Eq. (16) as

$$q = q_1 + q_2 \tag{21}$$

where q_1, q_2 satisfy

$$(\nabla^2 + \delta_1^2)q_1 = 0 \tag{22}$$

$$(\nabla^2 + \delta_2^2)q_2 = 0 \tag{23}$$

where

$$\delta_1^2 = \lambda_1^2\omega^2, \quad \delta_2^2 = \lambda_2^2\omega^2 \tag{24}$$

$$\lambda_{1,2}^2 = \frac{1}{2}(-A \pm \sqrt{A^2 - 4B}) \tag{25}$$

The roots of the Eqs. (22)-(23) correspond to longitudinal displacement wave and thermal wave propagating with velocities λ_1^{-1} (LD-wave) and λ_2^{-1} (T-wave).

We assume solution of Eq. (19) as

$$\psi = \psi_3 + \psi_4 \tag{26}$$

where ψ_3, ψ_4 satisfy

$$(\nabla^2 + \delta_3^2)\,\psi_3 = 0 \tag{27}$$

$$(\nabla^2 + \delta_4^2)\,\psi_4 = 0 \tag{28}$$

where

$$\delta_3^2 = \lambda_3^2\omega^2, \ \delta_4^2 = \lambda_4^2\omega^2 \tag{29}$$

$$\lambda_{3,4}^2 = \frac{1}{2}(-C \pm \sqrt{C^2 - 4D}) \tag{30}$$

The solution of Eqs. (27) and (28) correspond to two coupled transverse displacement and microrotationl waves propagating with velocities λ_3^{-1} (CD I-wave) and λ_4^{-1} (CD II-wave).

From Eq. (11), we obtain

$$T = a_1 q_1 + a_2 q_2 \tag{31}$$

where

$$a_i = \frac{1}{\upsilon}(-\delta_i^2(c_1^2 + c_3^2) + \omega^2), \qquad (i = 1, 2) \tag{32}$$

Eq. (12) can be written as

$$\phi_2 = E\,\psi_3 + F\,\psi_4 \tag{33}$$

where

$$E = \frac{1}{p}\left(\delta_3^2 - \frac{\omega^2}{c_2^2 + c_3^2}\right) \tag{34}$$

$$E = \frac{1}{p}\left(\delta_4^2 - \frac{\omega^2}{c_2^2 + c_3^2}\right) \tag{35}$$

The stress-displacement relation in elastic medium is given by

$$t'_{kl} = \lambda' u'_{r,r}\delta_{kl} + \mu'(u'_{k,l} + u'_{l,k}) \tag{36}$$

where symbols have their usual meaning.

For a homogeneous isotropic elastic solid, the Helmholtz resolution for the displacement

$$\vec{u}' = \text{grad}\phi' + \text{curl}\vec{\psi}' \tag{37}$$

the potentials are found to satisfy the wave equation

$$\nabla^2\phi' = \frac{1}{\alpha^2}\frac{\partial^2\phi'}{\partial t^2} \tag{38}$$

$$\nabla^2\psi' = \frac{1}{\beta^2}\frac{\partial^2\psi'}{\partial t^2} \tag{39}$$

where

$$\alpha^2 = (\lambda' + 2\mu')/\rho', \quad \beta^2 = \mu'/\rho', \quad \psi' = (\vec{\psi}')y \tag{40}$$

Since the problem is two-dimensional in *xz*-plane, therefore, we take

$$\vec{u}' = (u'_1, 0, u'_3) \tag{41}$$

the components of displacement in elastic medium.

4. Reflection and transmission

We consider micropolar thermoelastic wave (longitudinal displacement wave (LD-wave) or thermal wave (T-wave) or coupled transverse displacement and transverse microrotationl wave (CD I-wave) or coupled transverse displacement and transverse microrotationl wave (CD II-wave) propagating through the medium M which we designate as the region $z > 0$ and incident at the plane $z = 0$ with its direction of propagating with angle θ_0 normal to the surface. Corresponding to each incident wave, we get waves in medium M as reflected LD-, T-and CD I- and CD II-waves and transmitted P-wave and SV-wave in medium M'. We write all the variables without a prime in the region $z > 0$ (medium M as micropolar genarlized thermoelastic half-space) and attach a prime to denote the variables in the region $z < 0$ (medium M' as elastic half-space) as shown in Fig. (a).

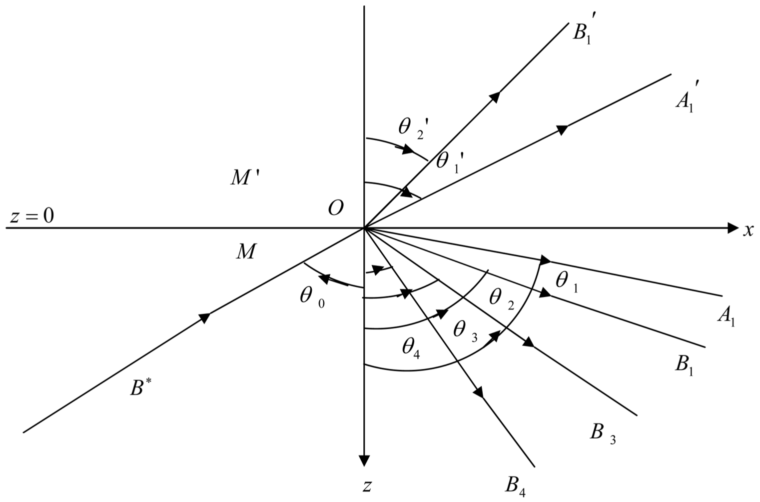

Fig. (a) Geometry of the problem

5. Boundary conditions

We consider two bonded elastic and micropolar generalized thermoelastic half spaces as shown in Fig. (a). If the bonding is imperfect and the size and spacing between the imperfections is much smaller than the wave-length then at the interface, these can be described by using boundary conditions at $z = 0$ (Lavrentyev and Rokhlin 1998) as

$$\begin{array}{ll} (1)\ (t_{33})_{M'} = K_n[(u_3)_M - (u_3)_{M'}] & (2)\ (t_{31})_{M'} = K_t[(u_1)_M - (u_1)_{M'}] \\ (3)\ (t_{33})_M = (t_{33})_{M'} & (4)\ (t_{31})_M = (t_{31})_{M'} \\ (4)\ (m_{32})_M = 0 & (4)\ \left(\dfrac{\partial T}{\partial z}\right) = 0 \end{array} \tag{42}$$

where K_n and K_t are normal force stiffness, transverse force stiffness coefficients of a unit layer thickness and having dimension N/m^3 each.

Appropriate potentials satisfying the boundary conditions (42) in medium M (micropolar generalized thermoelastic half-space) and M' (elastic half-space) can be written as

Medium M:

$$q = A_0\exp\{i\delta_1(x\sin\theta_0 - z\cos\theta_0) + i\omega_1 t\} + A_1\exp\{i\delta_1(x\sin\theta_1 + z\cos\theta_1) + i\omega_1 t\}$$
$$+ B_0\exp\{i\delta_2(x\sin\theta_0 - z\cos\theta_0) + i\omega_2 t\} + B_1\exp\{i\delta_2(x\sin\theta_2 + z\cos\theta_2) + i\omega_2 t\} \quad (43)$$

$$T = a_1A_0\exp\{i\delta_1(x\sin\theta_0 - z\cos\theta_0) + i\omega_1 t\} + a_1A_1\exp\{i\delta_1(x\sin\theta_1 + z\cos\theta_1) + i\omega_1 t\}$$
$$+ a_2B_0\exp\{i\delta_2(x\sin\theta_0 - z\cos\theta_0) + i\omega_2 t\} + a_2B_1\exp\{i\delta_2(x\sin\theta_2 + z\cos\theta_2) + i\omega_2 t\} \quad (44)$$

$$\psi = B_{03}\exp\{i\delta_3(x\sin\theta_{01} - z\cos\theta_{01}) + i\omega_3 t\} + B_3\exp\{i\delta_3(x\sin\theta_3 + z\cos\theta_3) + i\omega_3 t\}$$
$$+ B_{04}\exp\{i\delta_4(x\sin\theta_{01} - z\cos\theta_{01}) + i\omega_4 t\} + B_4\exp\{i\delta_4(x\sin\theta_4 + z\cos\theta_4) + i\omega_4 t\} \quad (45)$$

$$\phi_2 = EB_{03}\exp\{i\delta_3(x\sin\theta_{01} - z\cos\theta_{01}) + i\omega_3 t\} + EB_3\exp\{i\delta_3(x\sin\theta_3 + z\cos\theta_3) + i\omega_3 t\}$$
$$+ FB_{04}\exp\{i\delta_4(x\sin\theta_{01} - z\cos\theta_{01}) + i\omega_4 t\} + FB_4\exp\{i\delta_4(x\sin\theta_4 + z\cos\theta_4) + i\omega_4 t\} \quad (46)$$

Medium M':

$$q' = A_1'\exp\{i\delta_1'(x\sin\theta_1' - z\cos\theta_1') + i\omega_1' t\} \quad (47)$$

$$\psi' = B_2'\exp\{i\delta_2'(x\sin\theta_2' - z\cos\theta_2') + i\omega_2' t\} \quad (48)$$

where

$B_0, B_{03}, B_{04} = 0$ for incident longitudinal displacement wave (LD-wave)
$A_0, B_{03}, B_{04} = 0$ for incident thermal wave (T-wave)
$A_0, B_0, B_{04} = 0$ for incident coupled transverse displacement and transverse microrotationl wave (CD I-wave)
$A_0, B_0, B_{03} = 0$ for incident coupled transverse displacement and transverse microrotationl wave (CD II-wave)

Snell's law is given as

$$\frac{\sin\theta_0}{V_0} = \frac{\sin\theta_1}{\lambda_1^{-1}} = \frac{\sin\theta_2}{\lambda_2^{-1}} = \frac{\sin\theta_3}{\lambda_3^{-1}} = \frac{\sin\theta_4}{\lambda_4^{-1}} = \frac{\sin\theta_1'}{\alpha} = \frac{\sin\theta_2'}{\beta} \quad (49)$$

where

$$\delta_1(\lambda_1^{-1}) = \delta_2(\lambda_2^{-1}) = \delta_3(\lambda_3^{-1}) = \delta_4(\lambda_4^{-1}) = \delta_1'(\alpha) = \delta_2'(\beta) = \omega \quad \text{at } z = 0$$

and

$$V_0 = \begin{cases} \lambda_1^{-1} & \text{for incident longitudinal displacement wave (LD-wave)} \\ \lambda_2^{-1} & \text{for incident thermal wave (T-wave)} \\ \lambda_3^{-1} & \text{for incident a set of coupled transverse displacement and transverse microrotational wave (CD I-wave)} \\ \lambda_4^{-1} & \text{for incident a set of coupled transverse displacement and transverse microrotational wave (CD II-wave)} \end{cases}$$

Making use of potentials given by Eqs. (43)-(48) in boundary conditions (42) and with the help of Eqs. (1), (2), (7)-(10), (36), (37) and (41), we get a system of six non-homogeneous equations, which can be written as

$$\sum_{m=1}^{6} a_{mn} Z_n = Y_m \qquad (n = 1, 2, \ldots, 6) \tag{50}$$

where

$$a_{11} = -iK_n\delta_1\cos\theta_1, \quad a_{12} = -iK_n\delta_2\cos\theta_2, \quad a_{13} = -iK_n\delta_3\sin\theta_3$$
$$a_{14} = -iK_n\delta_4\sin\theta_4, \quad a_{15} = -(2\mu'\delta_1'^2\cos\theta_1'^2 + \lambda'\delta_1'^2 + iK_n\delta_1'\cos\theta_1')$$
$$a_{16} = 2\mu'\delta_2'^2\sin\theta_2'\cos\theta_2' + iK_n\delta_2'\sin\theta_2'$$
$$a_{21} = -iK_t\delta_1\sin\theta_1, \quad a_{22} = -iK_t\delta_2\sin\theta_2, \quad a_{23} = iK_t\delta_3\cos\theta_3$$
$$a_{24} = iK_t\delta_4\cos\theta_4, \quad a_{25} = 2\mu'\delta_1'^2\sin\theta_1'\cos\theta_1' + iK_t\delta_1'\sin\theta_1'$$
$$a_{26} = \mu'\delta_2'^2\cos\theta_2'^2 - \mu'\delta_2'^2\sin\theta_2'^2 + iK_t\delta_2'\cos\theta_2'$$
$$a_{31} = -((2\mu + K)\delta_1^2\cos\theta_1^2 + \lambda\delta_1^2 + \upsilon a_1), \quad a_{32} = -((2\mu + K)\delta_2^2\cos\theta_2^2 + \lambda\delta_2^2 + \upsilon a_2)$$
$$a_{33} = -(2\mu + K)\delta_3^2\sin\theta_3\cos\theta_3, \quad a_{34} = -(2\mu + K)\delta_4^2\sin\theta_4\cos\theta_4$$
$$a_{35} = 2\mu'\delta_1'^2\cos\theta_1'^2 + \lambda'\delta_1'^2, \quad a_{36} = -2\mu'\delta_2'^2\sin\theta_2'\cos\theta_2'$$
$$a_{41} = -(2\mu + K)\delta_1^2\sin\theta_1\cos\theta_1, \quad a_{42} = -(2\mu + K)\delta_2^2\sin\theta_2\cos\theta_2$$
$$a_{43} = (\mu + K)\delta_3^2\cos\theta_3^2 - \mu\delta_3^2\sin\theta_3^2 - KE$$
$$a_{44} = (\mu + K)\delta_4^2\cos\theta_4^2 - \mu\delta_4^2\sin\theta_4^2 - KF, \quad a_{45} = -2\mu'\delta_1'^2\sin\theta_1'\cos\theta_1'$$
$$a_{46} = -\mu'\delta_2'^2\cos\theta_2'^2 + \mu'\delta_2'^2\sin\theta_2'^2, \quad a_{51} = 0$$
$$a_{52} = 0, \quad a_{53} = \gamma E i\delta_3\cos\theta_3, \quad a_{54} = \gamma F i\delta_4\cos\theta_4, \quad a_{55} = 0, \quad a_{56} = 0$$
$$a_{61} = i\delta_1 a_1\cos\theta_1, \quad a_{62} = i\delta_2 a_2\cos\theta_2, \quad a_{63} = 0$$
$$a_{64} = 0, \quad a_{65} = 0, \quad a_{66} = 0$$

and

$$Z_1 = \frac{A_1}{B^*}, \ Z_2 = \frac{B_1}{B^*}, \ Z_3 = \frac{B_3}{B^*}, \ Z_4 = \frac{B_4}{B^*}, \ Z_5 = \frac{A_1'}{B^*}, \ Z_6 = \frac{A_2'}{B^*} \tag{51}$$

For incident longitudinal displacement wave (LD-wave): $B^* = A_0$

$$Y_1 = a_{11}, \ Y_2 = -a_{21}, \ Y_3 = -a_{31}, \ Y_4 = a_{41}, \ Y_5 = a_{51}, \ Y_6 = a_{61} \tag{52}$$

For incident thermal wave (T-wave): $B^* = B_0$

$$Y_1 = a_{12}, \ Y_2 = -a_{22}, \ Y_3 = -a_{32}, \ Y_4 = a_{42}, \ Y_5 = a_{52}, \ Y_6 = a_{62} \tag{53}$$

For incident coupled transverse displacement and transverse micrororational wave (CD I-wave) $B^* = B_{03}$

$$Y_1 = -a_{13}, \quad Y_2 = a_{23}, \quad Y_3 = -a_{33}, \quad Y_4 = -a_{43}, \quad Y_5 = a_{53}, \quad Y_6 = a_{63} \tag{54}$$

For incident coupled transverse displacement and transverse micrororational wave (CD II-wave): $B^* = B_{04}$

$$Y_1 = -a_{14}, \quad Y_2 = a_{24}, \quad Y_3 = a_{34}, \quad Y_4 = -a_{44}, \quad Y_5 = a_{54}, \quad Y_6 = a_{64} \tag{55}$$

where Z_1, Z_2, Z_3, Z_4, are amplitude ratio's of reflected longitudinal displacement wave (LD-wave) making an angle θ_1, thermal wave (T-wave) making angle θ_2 and a set of coupled transverse displacement and transverse microrotational waves (CD I- and CD II-waves) making an angle θ_3, θ_4 and Z_5, Z_6 are amplitude ratio's of transmitted P-wave making an angle θ_1' and SV-wave making an angle θ_2'.

6. Particular cases

CASE I: Normal Force Stiffness

$K_n \neq 0$ $K_t \to \infty$ correspond to the case of normal force stiffness and we obtain a system of six non-homogeneous equations as given by Eq. (50) with the changed values of a_{mn} as

$$a_{21} = \delta_1 \sin\theta_1, \quad a_{22} = \delta_2 \sin\theta_2, \quad a_{23} = -\delta_3 \cos\theta_3, \quad a_{24} = -\delta_4 \cos\theta_4$$
$$a_{25} = -\delta_1' \sin\theta_1', \quad a_{26} = -\delta_2' \cos\theta_2'$$

CASE II: Transverse Force Stiffness

$K_n \to \infty$ $K_t \neq 0$ the boundary conditions reduces to the transverse force stiffness, obtaining a system of six non-homogeneous equations as given by Eq. (50) with the modified values of a_{mn} as

$$a_{11} = \delta_1 \cos\theta_1, \quad a_{12} = \delta_2 \cos\theta_2, \quad a_{13} = \delta_3 \sin\theta_3, \quad a_{14} = \delta_4 \sin\theta_4$$
$$a_{15} = \delta_1' \cos\theta_1', \quad a_{16} = -\delta_2' \sin\theta_2'$$

CASE III: Welded Contact

$K_n \to \infty$ $K_t \to \infty$ correspond to the case of welded contact and we obtain a system of six non-homogeneous equations as given by Eq. (50) with the changed values of a_{mn} as

$$a_{11} = \delta_1 \cos\theta_1, \quad a_{12} = \delta_2 \cos\theta_2, \quad a_{13} = \delta_3 \sin\theta_3, \quad a_{14} = \delta_4 \sin\theta_4$$
$$a_{15} = \delta_1' \cos\theta_1', \quad a_{16} = -\delta_2' \sin\theta_2'$$
$$a_{21} = \delta_1 \sin\theta_1, \quad a_{22} = \delta_2 \sin\theta_2, \quad a_{23} = -\delta_3 \cos\theta_3, \quad a_{24} = -\delta_4 \cos\theta_4$$
$$a_{25} = -\delta_1' \sin\theta_1', \quad a_{26} = -\delta_2' \cos\theta_2'$$

7. Numerical results and discussion

Following Bullen (1963), we have the following values of density and elastic parameter for crust as elastic solid

$$\lambda' = 2.238 \times 10^{10}\ \text{Nm}^{-2},\ \mu' = 2.992 \times 10^{10}\ \text{Nm}^{-2}, \rho' = 2.65 \times 10^{3}\ \text{kgm}^{-3}$$

Following Eringen (1984), Dhaiwal and Singh (1980), we have the following values of density and micropolar thermoelastic parameters for Magnesium crystal as micropolar generalized thermoelastic solid

$$\lambda = 9.4 \times 10^{10}\ \text{Nm}^{-2}, \mu = 4.0 \times 10^{10}\ \text{Nm}^{-2}, K = 1.0 \times 10^{10}\ \text{Nm}^{-2}, \rho = 1.74 \times 10^{3}\ \text{kgm}^{-3}$$

$$\gamma = 0.779 \times 10^{-9}\ \text{N},\ j = 0.2 \times 10^{-19}\ \text{m}^2,\ \upsilon = 3.68 \times 10^{-6}\ \text{Nm}^{-2}\text{deg}^{-1},\ T = 298\ \text{K}$$

$$K^* = 1.7 \times 10^{2}\ J\text{sec}^{-1}\text{m}^{-1}\text{deg}^{-1},\ C^* = 1.04 \times 10^{3}\ J\text{kg}^{-1}\text{deg}^{-1}$$

with non-dimensional interface parameters as $\dfrac{K_n}{k\lambda} = 10,\ \dfrac{K_t}{k\lambda} = 20,\ \dfrac{\omega}{\omega_0'} = 1$ and $\omega_0' = \sqrt{\dfrac{K'}{\rho_j'}}$.

A computer programme has been developed and amplitude ratios of various reflected and transmitted waves has been computed. The variations of amplitude ratios for elastic solid/micropolar generalized thermoelastic solid with normal force stiffness (NS), elastic solid/micropolar generalized thermoelastic solid with transverse force stiffness (TS), elastic solid/generalized thermoelastic solid with normal force stiffness(NS) and elastic solid/generalized thermoelastic solid with transverse force stiffness (TS) have been shown by solid line, solid line with center symbol 'square', small dashed line and small dashed line with center symbol 'Triangle' respectively. The variations of the amplitude ratios $|Z_i| (i = 1, \ldots, 6)$ for elastic solid/micropolar generalized thermoelastic solid with normal force stiffness [ET/MGT(NS)], elastic solid/micropolar generalized thermoelastic solid with transverse force stiffness [ET/MGT(TS)], elastic solid/generalized thermoelastic solid with normal force stiffness [ET/GT(NS)]and elastic solid/generalized thermoelastic solid with transverse force stiffness [ET/GT(TS)] with angle of incidence θ_0 of the incident longitudinal displacement wave (LD-wave), incident thermal wave (T-wave), Incident coupled transverse displacement and microrotationl wave (CD I-wave) and incident coupled transverse displacement and microrotationl wave (CD II-wave) are shown graphically in Figs. 1-24.

(a) Incident longitudinal displacement wave (LD-wave):

The values of amplitude ratios $|Z_1|$ in case of ET/MGT (NS) show same trend of variations as in case of ET/MGT (TS) with difference in their magnitude in the whole range. The variations of amplitude ratios $|Z_1|$ in case of ET/GT (NS) are greater than ET/GT (TS) in the range $0^\circ \le \theta_0 \le 12^\circ$, $32^\circ \le \theta_0 \le 39^\circ$ and then have same variations in the remaining range. These variations are shown in Fig. 1.

The values of amplitude ratios $|Z_2|$ in case of ET/MGT (NS) and ET/MGT (TS) initially increase sharply and then decrease in the whole range. The variations of amplitude ratios $|Z_2|$ in case of ET/GT (NS) are greater than in case of ET/GT (TS) in the range $0^\circ \le \theta_0 \le 18^\circ$, $33^\circ \le \theta_0 \le 36^\circ$ and then have same behavior in the remaining range. These variations are shown in Fig. 2.

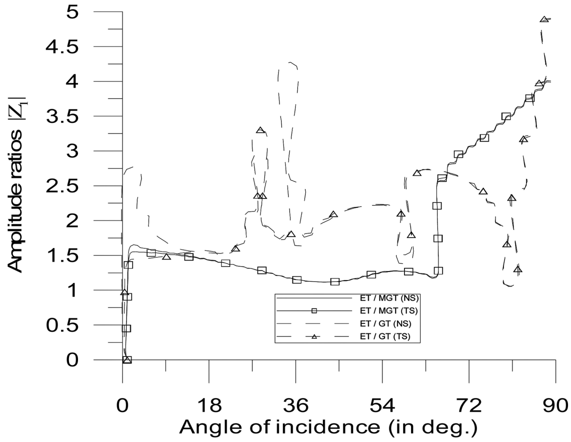

Fig. 1

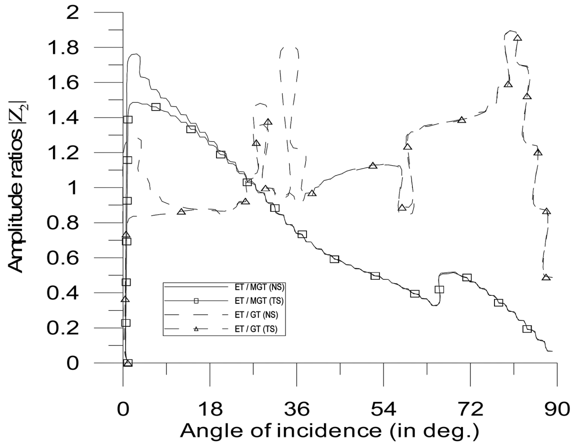

Fig. 2

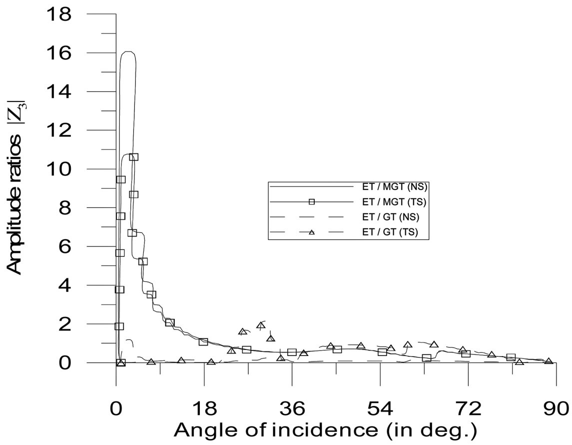

Fig. 3

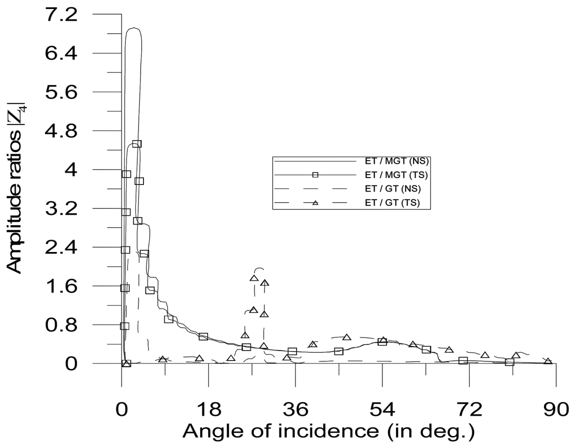

Fig. 4

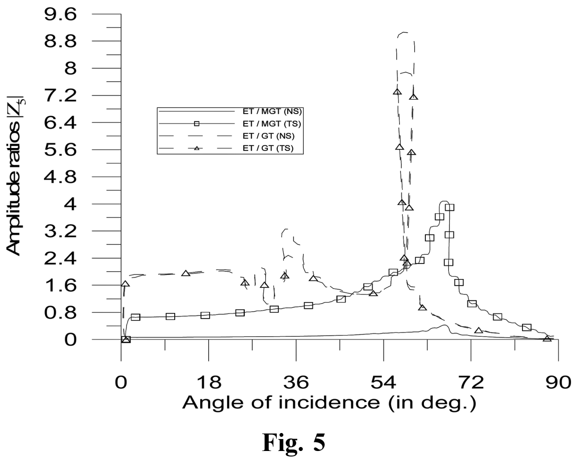

Fig. 5

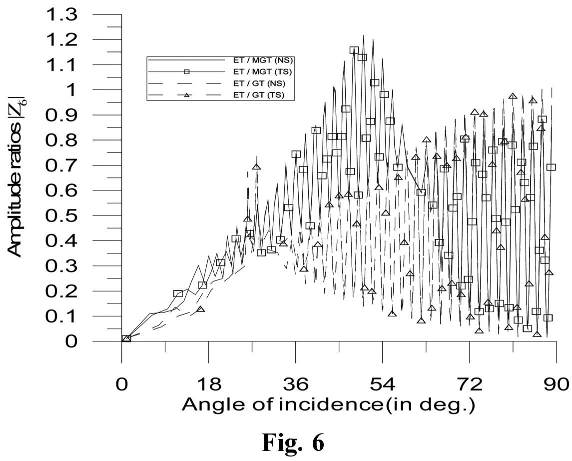

Fig. 6

Figs. 1-6 Variations of amplitude ratios with angle of incidence for LD-wave

The variations of amplitude ratios $|Z_3|$ in case of ET/MGT (NS) and ET/MGT (TS) increase sharply in the range $0^o \le \theta_0 \le 4^o$ and decrease sharply in the remaining range. The values of amplitude ratios $|Z_3|$ in case of ET/GT (TS) are smaller than in case of ET/GT (NS) in the range $0^o \le \theta_0 \le 7^o$, greater in the range $22^o \le \theta_0 \le 36^o$, $37^o \le \theta_0 \le 83^o$ and are close to each other in the remaining range. These variations are shown in Fig. 3.

It is observed from Fig. 4 that the values of amplitude ratios $|Z_4|$ in case of ET/MGT (NS) and ET/MGT (TS) increase sharply in the range $0^o \le \theta_0 \le 3^o$ and decrease sharply in the remaining range. The values of amplitude ratios $|Z_4|$ in case of ET/GT (TS) is greater than $|Z_4|$ in case of ET/GT (TS) in the range $22^o \le \theta_0 \le 90^o$ and have similar behavior in the remaining range.

The values of amplitude ratios $|Z_5|$ in case of ET/MGT (TS) are greater than in case of ET/MGT (NS) in the range $0^o \le \theta_0 \le 90^o$. The values of amplitude ratios $|Z_5|$ for ET/GT (NS) and ET/GT (TS) have same trend of variation except in the range $32^o \le \theta_0 \le 36^o$, $56^o \le \theta_0 \le 58^o$. These variations are shown in Fig. 5.

Fig. 6 shows that the values of amplitude ratios $|Z_6|$ for ET/MGT (NS), ET/MGT (TS), ET/GT (NS) and ET/GT (TS) increase in the range $0^o \le \theta_0 \le 18^o$ and then have an oscillatory behavior in the remaining range.

(b) Incident thermal wave (T-wave):

The values the amplitude ratios $|Z_1|$ in case of ET/MGT (NS) and ET/MGT (TS) increase in the range $0^o \le \theta_0 \le 63^o$ and decrease in the remaining range. The values of amplitude ratios $|Z_1|$ in case of ET/GT (NS) are greater than in case of ET/GT (TS) in the range $0^o \le \theta_0 \le 11^o$, $35^o \le \theta_0 \le 37^o$ and are close to each other in the remaining range. These variations are shown in Fig. 7.

Fig. 8 shows that the values of amplitude ratios $|Z_2|$ in case of ET/MGT (NS) and ET/MGT (TS) increase in the whole range. The variations of amplitude ratios $|Z_2|$ in case of ET/GT (NS) are greater than in case of ET/GT (TS) in the range $0^o \le \theta_0 \le 4^o$, $33^o \le \theta_0 \le 38^o$ and are very close to each other in the remaining range.

The values of amplitude ratios $|Z_3|$ in case of ET/MGT (NS) and ET/MGT (TS) increase in the range $0^o \le \theta_0 \le 4^o$ and decrease in the remaining range with difference in their magnitudes. The variations of amplitude ratios $|Z_3|$ in case of ET/GT (TS) are greater than ET/GT (NS) in the range $9^o \le \theta_0 \le 90^o$ and are smaller in the remaining range. These variations are shown in Fig. 9.

The variations of amplitude ratios $|Z_4|$ in case of ET/MGT (TS) are greater than in case of ET/MGT (NS) in the range $0^o \le \theta_0 \le 90^o$. The values of amplitude ratios $|Z_4|$ in case of ET/GT (NS) are greater than ET/GT (TS) in the range $0^o \le \theta_0 \le 11^o$ and are very close to each other in the remaining range. These variations are shown in Fig. 10.

It is observed from the Fig. 11 that the values of amplitude ratios $|Z_5|$ in case of ET/MGT (NS) and ET/MGT (TS) increase in the range $0^o \le \theta_0 \le 54^o$ and decrease in the remaining range. The values of amplitude ratios $|Z_5|$ in case of ET/GT (NS) and ET/GT (TS) have similar behavior in the whole range except in the range $33^o \le \theta_0 \le 38^o$.

The values of amplitude ratios $|Z_6|$ in case of ET/MGT (NS) and ET/MGT (TS) have an oscillatory behavior in the range $0^o \le \theta_0 \le 90^o$. The variations of amplitude ratios $|Z_6|$ in case of ET/GT (NS) and ET/GT (TS) increase in the range $0^o \le \theta_0 \le 25^o$ and have an oscillatory behavior in the remaining range. These variations are shown in Fig. 12.

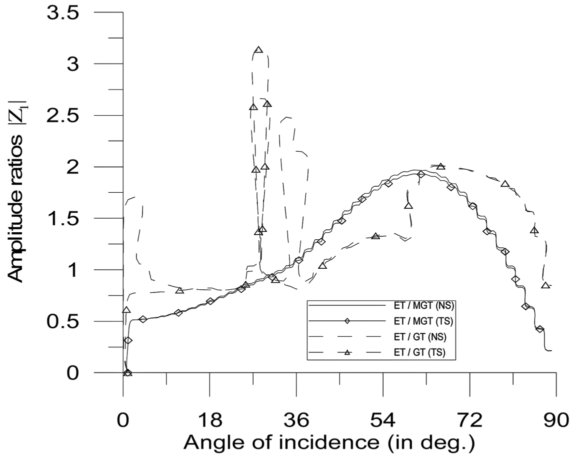

Fig. 7

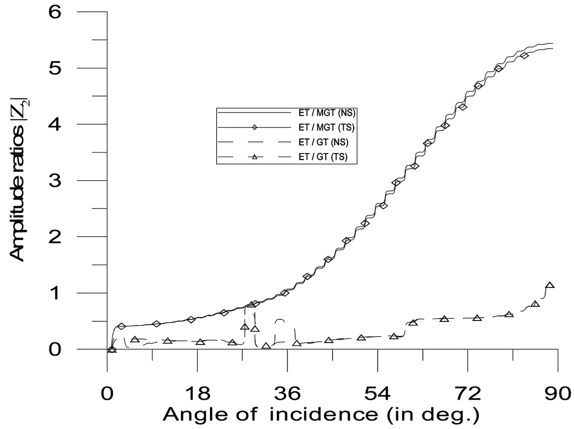

Fig. 8

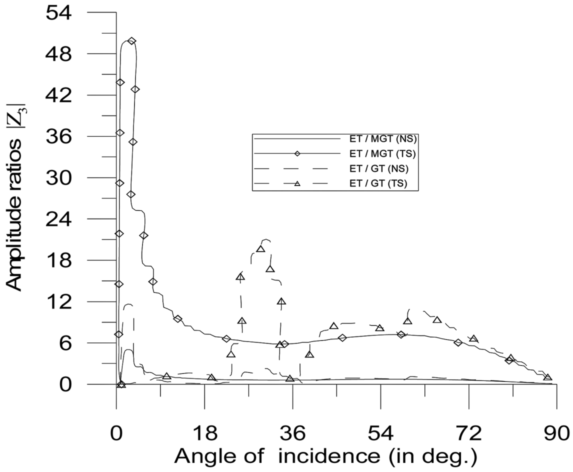

Fig. 9

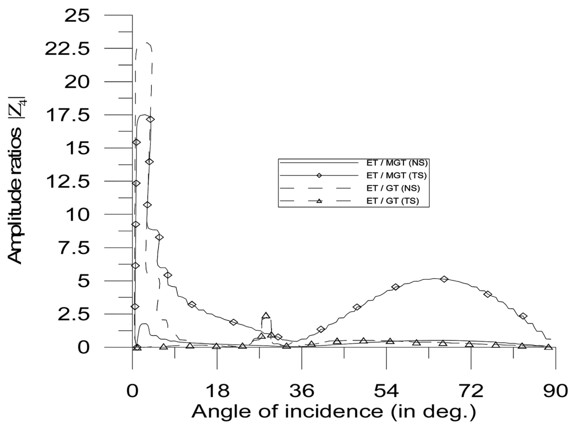

Fig. 10

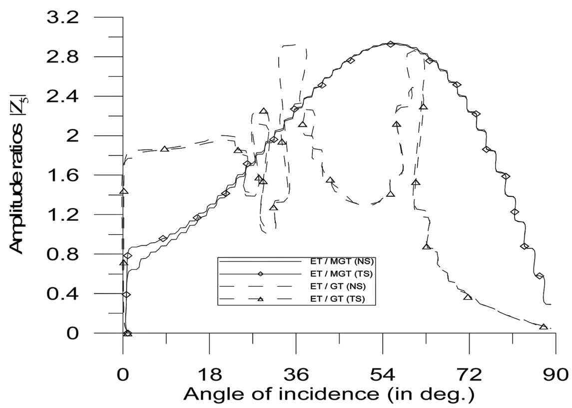

Fig. 11

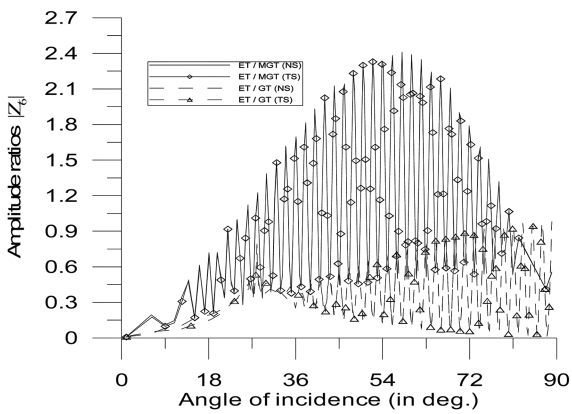

Fig. 12

Figs. 7-12 Variations of amplitude ratios with angle of incidence for T-wave

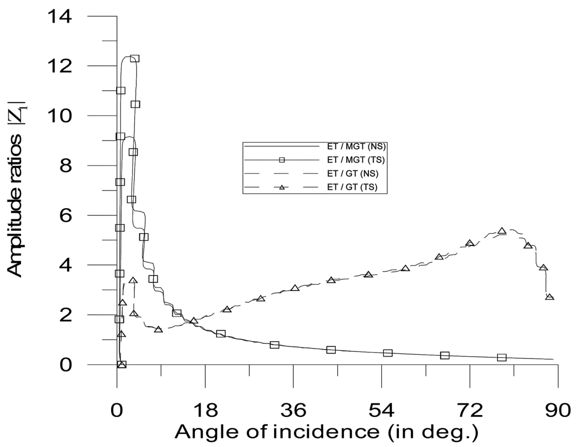

Fig. 13

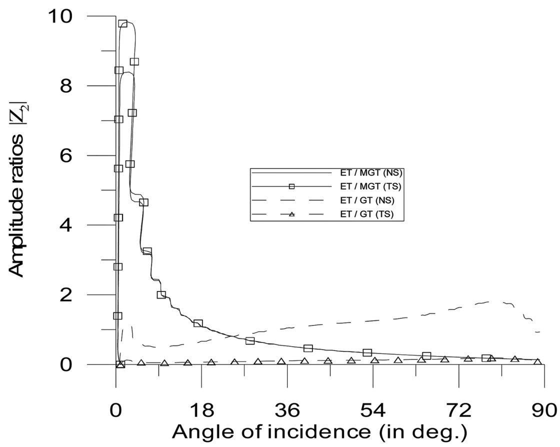

Fig. 14

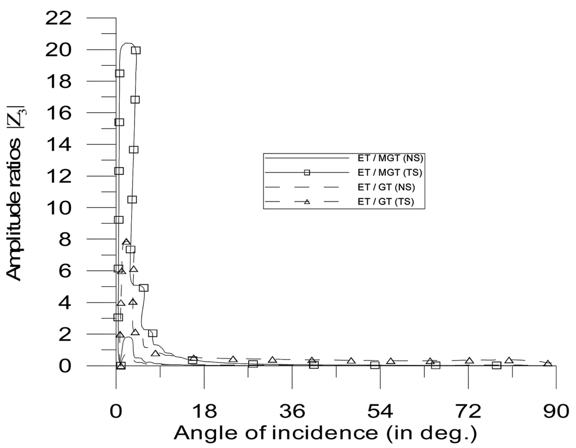

Fig. 15

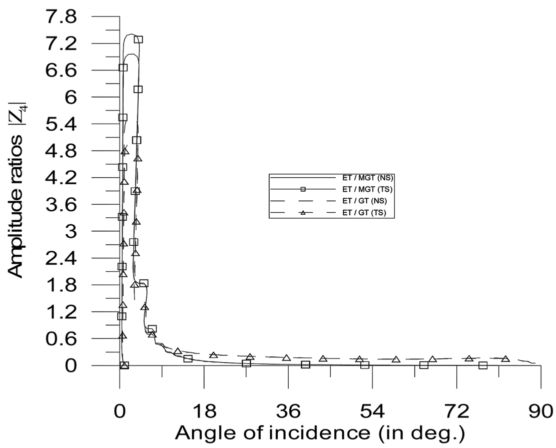

Fig. 16

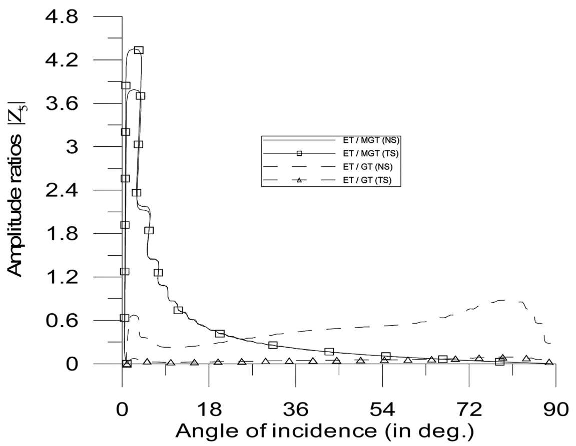

Fig. 17

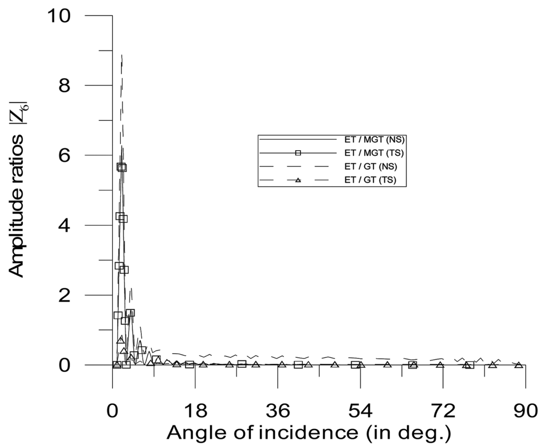

Fig. 18

Figs. 13-18 Variations of amplitude ratios with angle of incidence for CD-I wave

(c) Incident coupled transverse displacement and microrotationl wave (CD I-wave):

Fig. 13 shows that the values of amplitude ratios $|Z_1|$ in case of ET/MGT (NS) and ET/MGT (TS) initially increase and then decrease in the remaining range. The variations of amplitude ratios $|Z_1|$ in case of ET/GT (NS) and ET/GT (TS) increase in the whole range except $4^o \le \theta_0 \le 8^o$, $81^o \le \theta_0 \le 90^o$.

The values of amplitude ratios $|Z_2|$ in case of ET/MGT (NS) and ET/MGT (TS) initially increase in the range $0^o \le \theta_0 \le 4^o$ and then decrease in the remaining range. The values of amplitude ratios $|Z_2|$ in case of ET/GT (NS) are greater than ET/GT (TS) in the whole range $0^o \le \theta_0 \le 90^o$. These variations are shown in Fig. 14.

The values of amplitude ratios $|Z_3|$ in case of ET/MGT (NS), ET/MGT (TS) ET/GT (NS) and ET/GT (TS) initially increase with difference in their magnitudes and then decrease in the whole range. The values of amplitude ratios $|Z_3|$ are demagnified by dividing the original values by 10 in case of ET/GT (NS) and ET/GT (TS).These variations are shown in Fig. 15.

The values of amplitude ratios $|Z_4|$ shows same trend of variations as the values of amplitude ratios $|Z_3|$ (incident CD I-wave) with difference in their magnitudes. These variations are shown in Fig. 16.

The values of amplitude ratios $|Z_5|$ in case of ET/MGT (NS) and ET/MGT (TS) initially increase and then decrease in the remaining range. The values of amplitude ratios $|Z_2|$ in case of ET/GT (NS) are greater than ET/GT (TS) in the whole range $0^o \le \theta_0 \le 90^o$. These variations are shown in Fig. 17.

The values of amplitude ratios $|Z_6|$ in case of ET/MGT (NS), ET/MGT (TS) ET/GT (NS) and ET/GT (TS) have an oscillatory behavior in the range $0^o \le \theta_0 \le 18^o$ and then are very close to each other (near zero value). These variations are shown in Fig. 18.

(d) Incident coupled transverse displacement and microrotationl wave (CD II-wave):

The values of amplitude ratios $|Z_1|$ in case of ET/MGT (NS) and ET/MGT (TS) initially increase in the range $0^o \le \theta_0 \le 4^o$ and then decrease in the remaining range. The variations of amplitude ratios $|Z_1|$ in case of ET/GT (TS) are greater than ET/GT (NS) in the whole $0^o \le \theta_0 \le 90^o$. These variations are shown in Fig. 19.

It is observed from Fig. 20 that the values of amplitude ratios $|Z_2|$ in case of ET/MGT (NS) and ET/MGT (TS) initially increase in the range and then decrease in the remaining range. The values of amplitude ratios $|Z_2|$ in case of ET/GT (NS) and ET/GT (TS) increase in the range $0^o \le \theta_0 \le 4^o$. $12^o \le \theta_0 \le 54^o$, $63^o \le \theta_0 \le 81^o$ and decrease in the remaining range.

The values of amplitude ratios $|Z_3|$ in case of ET/MGT (NS), ET/MGT (TS) ET/GT (NS) and ET/GT (TS) initially increase and then decrease in the whole range. The values of amplitude ratios $|Z_3|$ are demagnified by dividing the original values by 10 in case of ET/GT (NS) and ET/GT (TS).These variations are shown in Fig. 21.

The values of amplitude ratios $|Z_4|$ shows same trend of variations as the values of amplitude ratios $|Z_3|$ (incident CD II-wave) with difference in their magnitudes. These variations are shown in Fig. 22.

Fig. 23 shows that the values of amplitude ratios $|Z_5|$ in case of ET/MGT (NS) and ET/MGT (TS) initially increase in the range $0^o \le \theta_0 \le 4^o$ and then decrease in the remaining range. The values of amplitude ratios $|Z_5|$ in case of ET/GT (NS) and ET/GT (TS) increase in the range $0^o \le \theta_0 \le 3^o$, $11^o \le \theta_0 \le 44^o$, $65^o \le \theta_0 \le 82^o$ and decrease in the remaining range.

The values of amplitude ratios $|Z_6|$ in case of ET/MGT (NS), ET/MGT (TS) ET/GT (NS) and ET/

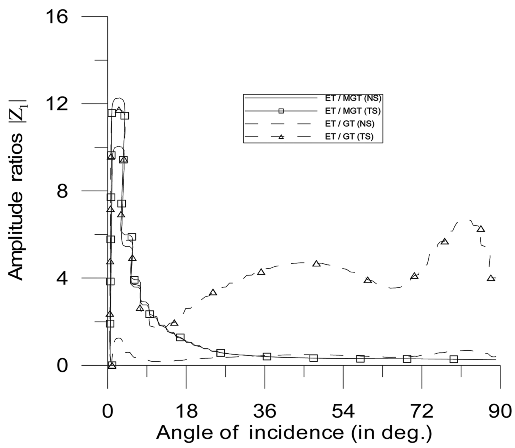

Fig. 19

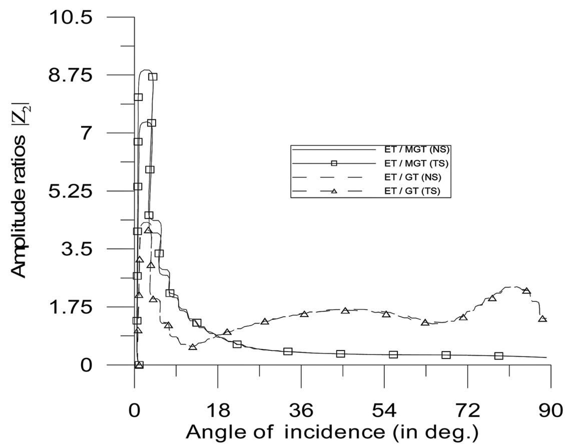

Fig. 20

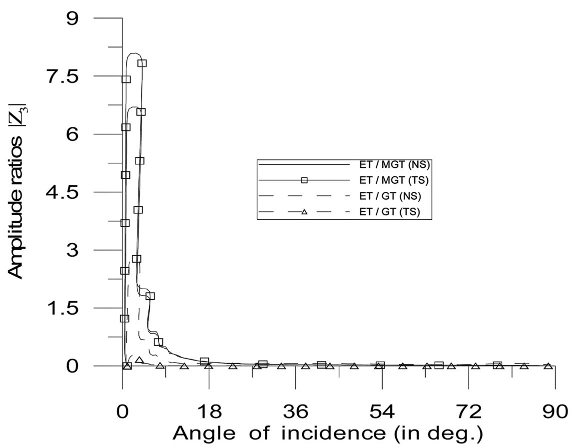

Fig. 21

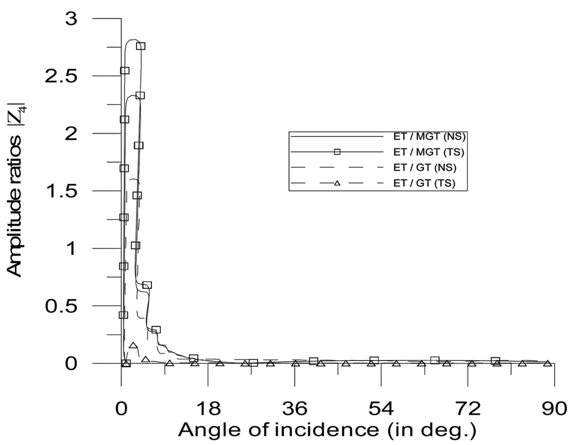

Fig. 22

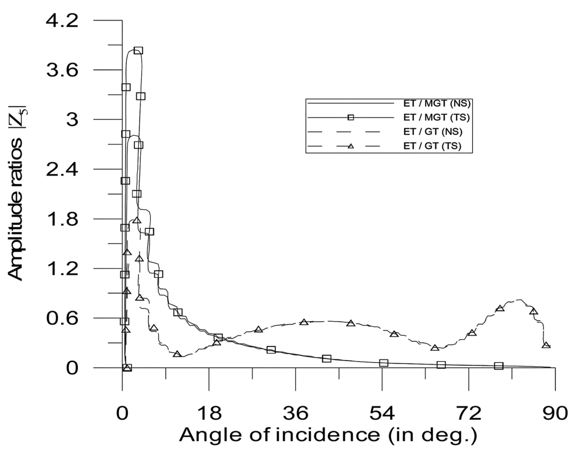

Fig. 23

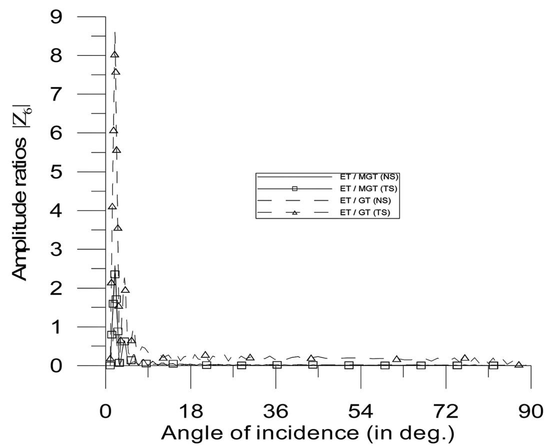

Fig. 24

Figs. 19-24 Variations of amplitude ratios with angle of incidence for CD-II wave

GT (TS) have an oscillatory behavior in the range $0^\circ \le \theta_0 \le 27^\circ$ and then show small variation near zero value. These variations are shown in Fig. 24.

8. Conclusions

Numerical calculations in detail have been presented for the case of LD-wave, T-wave, CD I-wave and CD II-wave incident at the interface of model considered. The theory of micropolar generalized thermoelasticity given by Eringen (1968) and Lord and Shulman (1999) has been used to solve the problem. The analytical expression for reflection and transmission coefficients of various reflected and transmitted waves have been derived for normal force stiffness, transverse force stiffness. It is observed that values of amplitude ratios in case of ET/MGT (NS), ET/MGT (TS) for $|Z_3|$, $|Z_4|$ and $|Z_6|$ have similar behavior with differences in magnitude for all values of θ_0 in case of incident LD-wave and T-wave. It is also observed that values of amplitude ratios for $|Z_3|$, $|Z_4|$, $|Z_5|$ and $|Z_6|$ in case of incident CD I-wave and incident CD II-wave shows same trend of variations with difference in their magnitudes. The model adopted in this paper is one of the more realistic forms of the earth models and it may be of interest for experimental seismologists. This problem, though theoretical, may be of some use in engineering, seismology and geophysics etc.

References

Angel, T.C. and Achenbach, J.D. (1985), "Reflection and transmission of elastic waves by a periodic array of crack", *J. Appl. Mech.*, **52**, 33-41.

Baik, J.M. and Thompson, R.B. (1984), "Ultrasonic Scattering from imperfect interfaces a quasi-static model", *J. Nondestruct. Eval.*, **4**, 177-196.

Boschi, E. and Iesan, D. (1973), "A generalized theory of linear micropolar thermoelasticity", *Meccanica*, **7**, 154-157.

Bullen, K.E. (1963), "An Introduction to theory of seismology, Cambridge University press, Cambridge.

Chen, W.Q., Cai, J.B., Ye, G.R. and Wang, Y.F. (2004), "Exact three-dimensional solutions of laminated orthotropic piezoelectric rectangular plates featuring interlaminar bonding imperfections modeled by a general spring layer", *Int. J. Solid Struct.*, **41**, 5247-5263.

Dhaliwal, R.S. and Singh, A. (1980), "Dynamical coupled thermoelasticity", Hindustan Publishers, Delhi.

Eringen, A.C. (1968), "Theory of micropolar elasticity 'in' Fracture", Chap. 7, Vol. II, Academic press, Newyork, Ed. H. Leibowitz.

Eringen, A.C. (1970), "Foundations of micropolar thermoelasticity", Int. Cent. for. Mech. Studies. Courses and Lectures, No.23, Springer-Verlag, Wien.

Eringen, A.C. (1984), "Plane waves in non-local micropolar elasticity", *Int. J. Eng. Sci.*, **22**, 1113-1121.

Eringen, A.C. (1999), "Microcontinuum field theory I: Fondations and solids", Springer-Verlag, Berlin.

Eringen, A.C. and Suhubi, E.S. (1964), "Non-linear theory of microelastic solids", I, II, *Int. J. Eng. Sci.*, **2**, 189-389.

Fan, H. and Sze, K.Y. (2001), "A micro-mechanics model for imperfect interface in dielectric materials", *Mech. Mater.*, **33**, 363-370.

Jones, J.P. and Whittier, J.S. (1967), "Waves in a flexible bounded interface", *J. Appl. Mech.*, **34**, 905-909.

Kumar, R. (2000), "Wave propagation in a micropolar viscoelastic generalized thermoelastic solid", *Int. J. Eng. Sci.*, **38**, 1377-1395.

Kumar, R. and Sarthi, P. (2006), "Reflection and refraction of thermoelastic plane waves at an interface between two thermoelastic media without energy dissipation", *Arch. Mech.*, **58**(2), 155-185.

Kumar, R. and Sharma, J.N. (2005), "Reflection of plane waves from the boundaries of a micropolar

thermoelastic half-space without energy dissipation", *Int. J. Appl. Mech. Eng.*, **10**(4), 631-645.
Kumar, R. and Singh, B. (1996), "Wave propagation in a micropolar generalized thermoelastic body with streach", *Proc. Indian Acad. Sci. (Math. Sci.)*, **106**, 183-199.
Kumar, R. and Singh, B. (1998), "Reflection of plane waves from the flat boundary of a micropolar generalized thermoelastic half-space", *Int. J. Eng. Sci.*, **36**, 865-890.
Kumar, R. and Singh, B. (1998), "Reflection of plane waves from the flat boundary of a micropolar generalized thermoelastic with streach", *Indian J. Pure. Ap. Ma.*, **29**, 657-669.
Kumar, R. and Singh, B. (1998), "Wave propagation in generalized thermo-microstrech elastic solid", *Int. J. Eng. Sci.*, **36**, 891-912.
Kumar, R., Sharma, N. and Ram, P. (2006), "Reflection and transmission of micrpolar elatic waves at an imperfect boundary", Multidiscipline Modeling in Materials and Structures (MMMS) [accepted].
Lavrentyev, A.I. and Rokhlin, S.I. (1998), "Ultrasonic spectroscopy of imperfect contact interfaces between a layer and two solids", *J. Acoust. Soc. Am.*, **103**(2), 657-664.
Murty, G.S. (1975), "A theoretical model for the attenuation and dispersion of stonely waves at the loosely bounded interface of elastic half-spaces", *Phys. Earth Planet. In.*, **11**, 65-79.
Nayfeh, A.H. and Nassar, E.M. (1978), "Simulation of the influence of bonding materials on the dynamic behaviour of laminated composites", *J. Appl. Mech.*, **45**, 822-828.
Nowacki, W. (1966), "Couple-stresses in the theory of thermoelasticity", In: Parkus, H., Sedov, L.I. (Eds.), Proc. IUTAM Symposia, Vienna, Springer-Verlag, 259-278.
Othman, M.I., Slalaeh, Oman and Song, Y. (2006), "The effect of rotation on the reflection of magneto-thermoelastic waves under thermoelasticity without energy dissipation", *Acta Mechanica*, **184**, 189-204.
Pilarski, A. and Rose, J.L. (1988), "A transverse wave ultrasonic oblique-incidence technique for interface weakness detection in adhesive bonds", *J. Appl. Phys.*, **63**, 300-307.
Rokhlin, S.I. (1984), "Adhesive joint characterization by ultrasonic surface and interface waves", Adhesive Joints: Formation, characteristics and testing. Edited by K.L. Mittal (plenum, New York), 307-345.
Rokhlin, S.I., Hefets, M. and Rosen, M. (1980), "An elastic interface waves guided by thin film between two solids", *J. Appl. Phys.*, **51**, 3579-3582.
Samsam Shariat, B.A. and Eslami, M.R. (2006), "Thermal buckling of imperfect functionally graded plates", *Int. J. Solid Struct.*, **43**, 4082-4096.
Schoenberg, M. (1980), "Elastic wave behaviour across linear slip interfaces", *J. Acoust. Soc. Am.*, **68**(5), 1516-1521.
Sharma, J.N., Kumar, V. and Chand, Dayal (2003), "Reflection of generalized thermoelastic waves from the boundary of a half-space", *J. Therm. Stresses*, **26**, 925-942.
Shodja, H.M., Tabatabaei, S.M. and Kamali, H.T. (2006), "A Piezoelectric-inhomogenity system with imperfect interface", *Int. J. Eng. Sci.*, **44**, 291-311.
Sotiropoulos, D.A. and Achenbach, J.D. (1988), "Ultrasonic reflection by planar distribution of cracks", *J. Nondestruct. Eval.*, **7**, 23-129.
Wang, X. and Zhong, Z. (2003), "Three-dimensional solution of smart laminated anisotropic circular cylindrical shellswith imperfect bonding", *Int. J. Solid Struct.*, **40**, 5901-5921.